Contents lists available at ScienceDirect

Genomics Data

Data in Brief

Association of aging with gene expression profiling in mouse submandibular glands

CrossMark

Yoshiro Saito [a,b], Atsushi Yamada [a,*], Dai Suzuki [a], Junichi Tanaka [c], Ryo Nagahama [a,d], Tamaki Kurosawa [a], Koutaro Maki [d], Kenji Mishima [c], Tatsuo Shirota [a], Ryutaro Kamijo [a]

[a] Department of Biochemistry, School of Dentistry, Showa University, Shinagawa, Tokyo 142-8555, Japan
[b] Department of Oral and Maxillofacial Surgery, School of Dentistry, Showa University, Ohta, Tokyo 145-8515, Japan
[c] Department of Oral Diagnostic Sciences, School of Dentistry, Showa University, Shinagawa, Tokyo 142-8555, Japan
[d] Department of Orthodontics, School of Dentistry, Showa University, Ohta, Tokyo 145-8515, Japan

ARTICLE INFO

ABSTRACT

Aging, also called senescence, is thought to be a physiological phenomenon that commonly occurs in various organs and tissues (Enoki et al., 2007 [1]). Many older adults experience dysfunction in their salivary glands, for example xerostomia, which is defined as dry mouth resulting from reduced or absent saliva flow (Nagler et al., 2004 [2]). In the present study, we investigated gene expression in submandibular glands of young (8 weeks old) and adult (50 weeks old) mice to analyze association of aging with gene expression profiling in mouse submandibular glands. Whole-genome gene expression profiles were analyzed using an Illumina Sentrix system with Mouse-WG-6 v.2 Expression BeadChips (Illumina). Of the genes screened, 284 showed detection values at a significance level of $P < 0.01$. Among those, the expression of 94 genes (33%) showed a greater decrease in adult mice as compared to young mice. On the other hand, that of 190 genes (77%) was increased in the adults more than in young mice. The data obtained in this study are publicly available in the Gene Expression Omnibus (GEO) database (accession number GSE66857).

Specifications

Organism/cell line/tissue	*Mus musculus*/submandibular glands of young (8 weeks old) and adult (50 weeks old) mice
Sex	Male
Sequencer or array type	Illumina Mouse-WG-6 v.2 expression bead chip
Data format	Raw and analyzed
Experimental factors	Expression patterns in submandibular glands of young (8 weeks old) and adult (50 weeks old) mice were analyzed to determine aging-dependent gene expression.
Experimental features	Microarray analysis of gene expression associated with aging in mouse submandibular glands.
Consent	N/A
Sample source location	1-5-8 Hatanodai, Shinagawa, Tokyo 142-8555, Japan

* Corresponding author at: Department of Biochemistry, School of Dentistry, Showa University, 1-5-8 Hatanodai, Shinagawa, Tokyo 142-8555, Japan. Tel.: +81 3 3784 8163; fax: +81 3 3784 5555.
 E-mail address: yamadaa@dent.showa-u.ac.jp (A. Yamada).

1. Direct link to deposited data

http://www.ncbi.nlm.nih.gov/geo/query/acc.cgi?acc=GSE66857.

2. Experimental design, materials, and methods

2.1. Introduction

The submandibular glands (SMGs) participate as major salivary secreting organs to secrete fluids rich in proteins that are critical for maintenance of oral health [1-3]. The SMGs have been reported to increase in proportional volume of fat and connective tissues with a reduction in that of acini with aging, though without any remarkable change in the volume of the duct system [4]. For investigation of age-dependent changes in the expression of genes in SMGs, a gene expression array can provide a comprehensive view of the expression pattern. The Illumina Sentrix system using Mouse-WG-6 v.2 Expression BeadChips (Illumina) reflects the latest advancements in mouse genomics and provides biologically relevant information for gene expression studies, while GenomeStudio Data Analysis Software is useful for visualizing and analyzing data obtained with the

Table 1
Sequences of primers used for quantitative PCR.

Gene	Primer	Sequence
Pdcd4	Forward	5′-GGATGAGACCGCATTTGAGAA-3′
	Reverse	5′-AGGCTAAGGACACTGCCAACAC-3′
Ttr	Forward	5′-GGTCAAAGTCCTGGATGCTGTC-3′
	Reverse	5′-CCAGTACGATTTGGTGTCCAGTTC-3′
Pdk4	Forward	5′-CAGGTTATGGGACAGACGCTATCA-3′
	Reverse	5′-TGCTTGGGATACACCAGTCATCA-3′
Ly6d	Forward	5′-CCAGCAGGGCCATGTCA-3′
	Reverse	5′-AGGTCAGTCTGGCAGCATTGT-3′
Kik1	Forward	5′-TGACAGATGACATGTTGTGTGCAG-3′
	Reverse	5′-GATACCCGGCACATTGGGTTTA-3′
Creld2	Forward	5′-GCGATGGCCAGTACTGTGAGAA-3′
	Reverse	5′-CTGTACAGCCCACGCAGGTAGA-3′
Igfbp2	Forward	5′-GGCCGGTACAACCTTAAGCA-3′
	Reverse	5′-GGGTTCACACACCAGCACTC-3′
Sdf2l1	Forward	5′-GCTGCACTCACACGACATCAA-3′
	Reverse	5′-CGCGAATCCGCCAGTAACTA-3′
Tgm2	Forward	5′-CAACCTGACCCTGGATCCCTA-3′
	Reverse	5′-TCAGGCACCCGCTGTACTTC-3′

Illumina array platform. In the present study, we used cDNA micro-array analysis to detect age-associated changes in gene expression of mouse SMGs.

2.2. Animal treatment

All animal experiments were conducted in accordance with the guidelines of Showa University. C57BL/6J mice were obtained from Sankyo Laboratory and housed in the Animal Facility at Showa University. We used 8- and 50-week-old mice as the young and adult, respectively, groups.

2.3. Tissue preparation

For general histopathological examinations, all samples were fixed in 4% paraformaldehyde and processed into frozen sections using routine procedures, then stained with hematoxylin–eosin (H–E).

2.4. Whole-genome expression assay and microarray data analysis

Whole-genome gene expression profiles in the SMGs of each mouse were analyzed using an Illumina Sentrix system with Mouse-WG-6 v.2 Expression BeadChips (Illumina), which includes 45,281 Illumina probes to detect transcriptants covering 30,854 genes, using a previously reported method [5]. First, total RNA was extracted with TRIzol reagent (Life Technologies) from whole SMGs, then 500 ng was subjected to RNA amplification, which was performed with an Illumina TotalPrep RNA Amplification Kit (Ambion), according to the manufacturer's instructions. Biotinylated cRNA was then hybridized to Mouse-WG-6 v.2 Expression BeadChips and reacted with streptavidin-cy3 (GE Healthcare). Finally, the expression intensity of the transcripts on the BeadChips was detected using an Illumina iScan reader. Raw BeadChip image data were subjected to expression analyses using the manufacturer's software (GenomeStudio v.2011.1, Gene Expression Module v.1.9.0). A heat map was generated by hierarchical clustering of the selected transcripts based on the gene expression profiles (expression ratio: AVG_signal of adult mice/AVG_signal of young mice).

2.5. Quantitative real-time PCR

Total RNA was extracted using TRIzol reagent (Life Technologies), then reverse transcribed using ReverTra Ace® qPCR RT Master Mix (TOYOBO). Quantitative real-time PCR was performed using a SYBR green Fast PCR system (GE Healthcare), with the following primer sequences shown in Table 1.
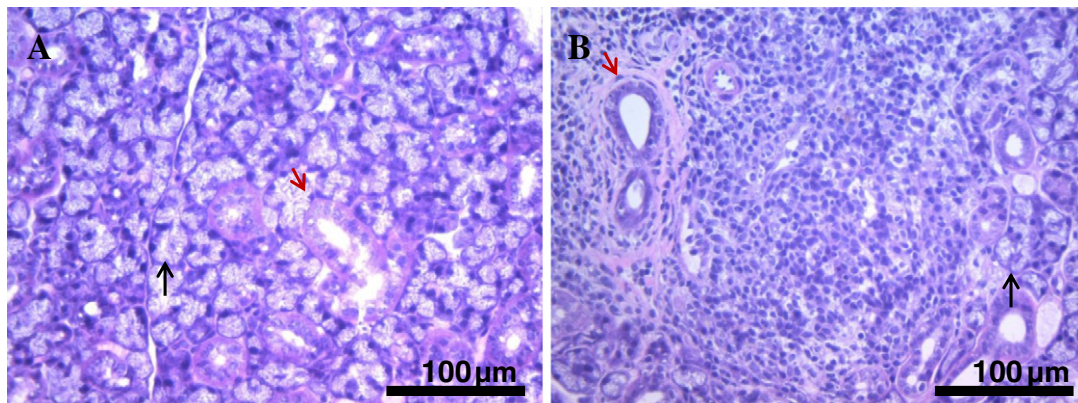
Fig. 1. Representative sections from submandibular glands of young and adult mice (H & E, scale bars: 100 μm). Black arrows, acinar cell; red arrows, duct.

A

AVG_Signal
young vs. adult mice

B

C

Category	No. of genes
Transcription regulation	50
Ribosome biogenesis	6
Structure protein	2
Membrane protein	20
Proteolysis and peptidolysis	8
Protein folding	1
Enzyme	36
Cytoskeleton	13
Signal transduction	47
Transport	6
Metabolism	14
Immunity	17
Matrix	7
Cell cycle	1
Channel	1
Others	55
	284
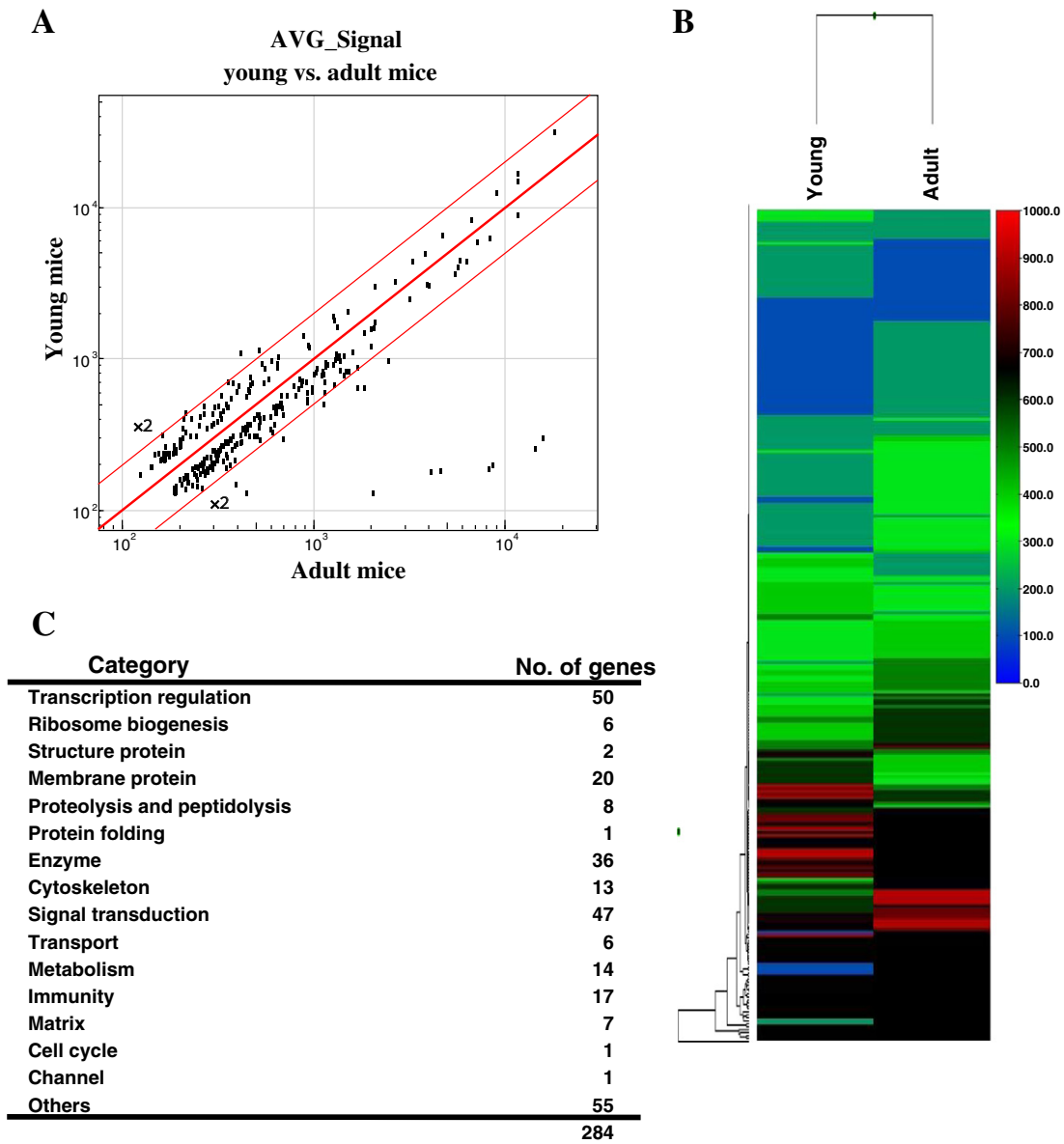
Fig. 2. Genome wide gene expression profiling of submandibular glands from C57BL/6J mice at 8 (young) and 50 (adult) weeks old. Biotinylated cRNA was synthesized from total RNA and hybridized to Illumina MouseWG-6 v.2 Expression BeadChips. Raw expression intensity data were analyzed using GenomeStudio Software. (A) Scatterplots of the AVE_Signal for young and adult mice were generated. (B) Heat map illustration of gene expression profiles in young and adult mice. Hierarchical clustering was based on relative gene expression levels (AVG_Signal/AVG_Signal of C57BL/6J mouse). (C) Selected 284 transcript expression changes among young and adult mice based on whole-genome expression analysis.

3. Results and discussion

SMGs in both the young and adult mice consisted of acini, a duct system, and interstitial connective tissues. The nuclei of the acinar cells were restricted to the basal side, where cytoplasm filled clear granules in both phenotypes. In the young mice, duct cells as well as intercalated, granular, striated, and excretory cells were clearly identified in the duct system of the SMGs (Fig. 1A). On the other hand, histological findings of those from adult mice showed mainly periductal inflammation of lymphocytes in the SMGs and inflammatory cell infiltration leading to destruction of acini (Fig. 1B).

To elucidate the molecular mechanisms of changes associated with age in the mice, we performed whole-genome expression assays using the Illumina Sentrix platform with Mouse WG-6 v.2 Expression BeadChips. Obtained raw signal intensity data were analyzed using GenomeStudio Software. Following baseline subtraction and normalization, among the 45,281 transcripts of all detected genes, 284 showed an expression detection significance of $P < 0.01$. The expression levels of those 284 transcripts differed between the young and adult mice. Scatterplots for both groups displayed a symmetrical AVG_Signal distribution around linear identity lines to form a 45° angle. The expression levels of 3 genes in the adult mice showed a greater than two-fold reduction, while those of 12 genes showed a greater than two-fold increase (Fig. 2A). Of the 284 transcripts, 94 exhibited lower and 190 exhibited higher expression in adults as compared to the young mice (Fig. 2B). The categories of the altered genes are shown in Fig. 2C. Of the 284 genes, 50 (17.6%)

Table 2

Highly differentially expressed gene profiles in submandibular glands from young and adult mice. Genes noted by *red font* were subjected to quantitative real-time PCR analysis.

Probe ID	Symbol	Signal intensity		Fold change
		Young mice	Adult mice	
ILMN_2898878	Pdcd4	1078	413.4	0.38
ILMN_2443330	Ttr	1143	523.7	0.46
ILMN_2803920	Ly6d	441.2	213.8	0.48
ILMN_1243212	Sparc	693.5	361.2	0.52
ILMN_1259322	Pdk4	395.3	209.9	0.53
ILMN_1258629	Col3a1	482.5	268.6	0.56
ILMN_2660466	EG433229	679.9	379.4	0.56
ILMN_2747923	Slc40a1	396.1	229.8	0.58
ILMN_2949021	Aadacl1	569.1	331.3	0.58
ILMN_3136561	Sparc	924	537.9	0.58
ILMN_2760199	Klk1	31322	18240	0.58
ILMN_2810882	Ppic	345.7	208.5	0.6
ILMN_3150811	Tsc22d3	763.7	468	0.61
ILMN_2691996	Ascl3	661.9	408.4	0.62
ILMN_1221501	5730469M10Rik	973.3	600.5	0.62
ILMN_2499264	4933428A15Rik	414.6	256.7	0.62
ILMN_2687872	Col1a1	430.5	268.4	0.62
ILMN_1257299	G0s2	1418	885	0.62
ILMN_2898578	Atp6v1c2	474.9	303.2	0.64
ILMN_2729103	Adamts2	1030	658.5	0.64
ILMN_2637094	Pcsk6	232.9	149	0.64
ILMN_2761436	Aldh1a3	261.4	169.1	0.65
ILMN_2599449	Abpg	855.9	556.5	0.65
ILMN_2437848	Col4a5	237.6	155.2	0.65
ILMN_1226259	Adamts2	609.2	398.3	0.65
ILMN_2670398	Eif4ebp1	1928	1271	0.66
ILMN_1245043	LOC226017	324.5	215.5	0.66
ILMN_2795698	Paox	546	370.8	0.68
ILMN_3052781	Slc25a34	268.5	186	0.69
ILMN_1240264	Usp2	429.3	297.8	0.69
ILMN_2704562	LOC100047628	255.1	14370	56.34
ILMN_2684370	Igk–C	298.1	15863	53.21
ILMN_2744660	Igh–6	184.6	8241	44.63
ILMN_2635272	Igh–VJ558	182.9	4595	25.12
ILMN_1245146	Igl–V1	178.9	4108	22.96
ILMN_2772264	Igh–VJ558	130	2044	15.73
ILMN_1248316	Ptgds	128.9	445.3	3.45
ILMN_2940642	St6galnac2	641.8	1844	2.87
ILMN_1239102	H2–Eb1	651.6	1703	2.61
ILMN_2607675	LOC641240	958.9	2458	2.56
ILMN_2776034	Gal	293.6	698.9	2.38
ILMN_2913716	H2–Ab1	495.2	1135	2.29
ILMN_2964324	Igfbp5	668.2	1284	1.92
ILMN_2757368	Creld2	595.8	1146	1.92
ILMN_1232265	LOC331239	877	1688	1.92
ILMN_1258526	Lgals3bp	327.6	611.1	1.87
ILMN_2699665	Cd209f	140.3	262	1.87
ILMN_1242466	Psmb9	196.1	366	1.87
ILMN_2795412	Tmem176a	769.5	1438	1.87
ILMN_2930897	Igfbp2	191	352.5	1.85
ILMN_2983948	Creld2	828	1525	1.84
ILMN_1221943	Sdf2l1	290.6	524.9	1.81
ILMN_1259564	Iigp2	215.3	387.3	1.8
ILMN_2839313	Actg2	337.6	597.5	1.77
ILMN_2692615	Tgm2	520.5	922.9	1.77
ILMN_2725927	Serpina3g	142.8	245.5	1.72
ILMN_2954868	Oasl2	370.9	625	1.69
ILMN_2658501	Ifitm3	1207	2016	1.67
ILMN_1224855	Samd9l	308.7	509.6	1.65
ILMN_2728134	5430433G21Rik	422.8	692.6	1.64
ILMN_2682613	Igfbp5	699.5	1147	1.64
ILMN_2667091	Ppp1r3c	839.2	1372	1.63
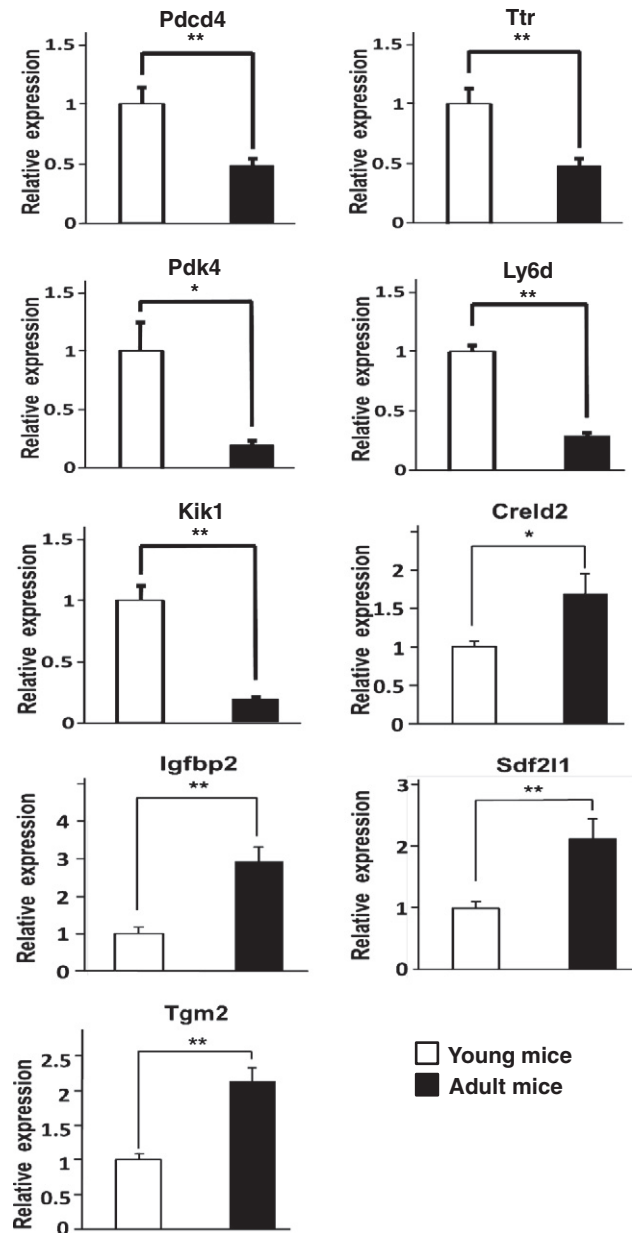
Fig. 3. Quantitative PCR analysis. Results are shown as the mean ± SEM of 6 samples. *P < 0.05, **P < 0.0; Student's t test.

encode transcription regulation, 47 (16.5%) encode signal transduction, 36 (12.7%) encode enzymes, and 17 (6%) encode immunity. Table 2 shows the 30 genes with lower (<0.69) and 32 genes with higher (>1.63) fold changes in expression level in the adults as compared to the young mice. To verify the microarray data, 9 genes (*red* in Table 2) were randomly selected and quantitative PCR was performed (Fig. 3), with the results consistent with the microarray findings.

Among the 9 picked-up genes, Pdcd4 (Programmed cell death 4) is characterized as a potent tumor suppressor and known to inhibit the function of transcription factors, such as AP-1 transactivation [6–8]. Furthermore, Hayashi et al. demonstrated that miR-21, whose target gene is Pdcd4 and regulates branching morphogenesis in the submandibular glands [8]. In the present study, Pdcd4 was decreased in the SMGs of adult mice. Additional experiments are required to fully elucidate the mechanism involved in that decrease.

Conflict of interest

The authors declare that there are no potential conflicts of interest with respect to the authorship and/or publication of this article.

Acknowledgments

References

[1] N. Enoki, T. Kiyoshima, T. Sakai, I. Kobayashi, K. Takahashi, Y. Terada, H. Sakai, Age-dependent changes in cell proliferation and cell death in the periodontal tissue and the submandibular gland in mice: a comparison with other tissues and organs. J. Mol. Histol. 38 (2007) 321–332.

[2] R.M. Nagler, Salivary glands and the aging process: mechanistic aspects, health-status and medicinal-efficacy monitoring. Biogerontology 5 (2004) 223–233.

[3] C.Q. Nguyen, A. Sharma, B.H. Lee, J.X. She, R.A. McIndoe, A.B. Peck, Differential gene expression in the salivary gland during development and onset of xerostomia in Sjogren's syndrome-like disease of the C57BL/6.NOD-Aec1Aec2 mouse. Arthritis Res. Ther. 11 (2009) R56.

[4] H. Suzuki, N. Amizuka, M. Noda, O. Amano, T. Maeda, Histological and immunohisto-chemical changes in the submandibular gland in klotho-deficient mice. Arch. Histol. Cytol. 69 (2006) 119–128.

[5] S. Kasai, K. Ikeda, Reduced supraspinal nociceptive responses and distinct gene expression profile in CXBH recombinant inbred mice. J. Pain 14 (2013) 648–661.

[6] A.M. Krichevsky, G. Gabriely, miR-21: a small multi-faceted RNA. J. Cell. Mol. Med. 13 (2009) 39–53.

[7] H.S. Yang, A.P. Jansen, R. Nair, K. Shibahara, A.K. Verma, J.L. Cmarik, N.H. Colburn, A novel transformation suppressor, Pdcd4, inhibits AP-1 transactivation but not NF-kappaB or ODC transactivation. Oncogene 20 (2001) 669–676.

[8] T. Hayashi, N. Koyama, Y. Azuma, M. Kashimata, Mesenchymal miR-21 regulates branching morphogenesis in murine submandibular gland in vitro. Dev. Biol. 352 (2011) 299–307.